J. Membrane Biol. 193, 185–194 (2003)
DOI: 10.1007/s00232-003-2017-9

The Journal of
Membrane
Biology

Monovalent Cations Contribute to T-type Calcium Channel ($Ca_V3.1$ and $Ca_V3.2$) Selectivity

B.P. Delisle*, J. Satin
Department of Physiology, The University of Kentucky College Medicine, 800 Rose St., Lexington, KY 40536-0298, USA

Received: 5 September 2002/Revised: 24 February 2003

Abstract. Low voltage-activated (LVA) Ca^{2+} channels regulate chemical signaling by their ability to select for Ca^{2+}. Whereas Ca^{2+} is the main permeating species through Ca^{2+} channels, Ca^{2+} permeation may be modified by abundant intra- and extracellular monovalent cations. Therefore, we explored monovalent cation regulation of LVA Ca^{2+} permeation in the cloned T-type Ca^{2+} channels α1G ($Ca_V3.1$) and α1H ($Ca_V3.2$). In physiological [Ca^{2+}], the reversal potential in symmetrical Li^+ was 19 mV in α1G and 18 mV in α1H, in symmetrical Cs^+ the reversal potential was 36 mV in α1G and 37 mV in α1H, and in the bi-ionic condition with Li^+ in the bath and Cs^+ in the pipette, the reversal potential was 46 mV in both α1G and α1H. When Cs^+ was used in the pipette, replacement of external Cs^+ with Li^+ (or Na^+) shifted the reversal potential positive by 5–6 mV and increased the net inward current in α1G. Taken together the data indicate that in physiological [Ca^{2+}], external Li^+ (or Na^+) permeates more readily than external Cs^+, resulting in a positive shift of the reversal potential. We conclude that external monovalent cations dictate T-type Ca^{2+} channel selectivity by permeating through the channel. Similar to Li^+, we previously reported that external [H^+] can regulate T-type Ca^{2+} channel selectivity. α1H's selectivity was more sensitive to external pH changes compared to α1G. When Cs^+ was used in the pipette and Li^+ was used in the bath external acidification from pH_o 7.4 to 6.0 caused a negative shift of the reversal by 8 mV in α1H. Replacement of internal Cs^+ with Li^+ reduced the pH-induced shift of the reversal potential to 2 mV. We conclude that, similar to other external monovalent cations, H^+ can modify T-type Ca^{2+} channel selectivity. However, in contrast to external monovalent ions that readily permeate, H^+ regulate T-type Ca^{2+} channel selectivity by increasing the relative permeability of the internal monovalent cation.

Key words: Calcium channel — Low-voltage-activated channel — Ion permeation — Selectivity — Patch-clamp

Introduction

Voltage-gated calcium channels (VGCC) are critical components of electrical and biochemical signaling in neurons, myocytes, and endocrine cells. Ca^{2+} channels are of prime importance because of the role Ca^{2+} plays in contraction, secretion, and in the regulation of second messenger pathways (Hille, 2001). There are two distinct classes of VGCC, low-voltage-activated (LVA) and high-voltage-activated (HVA) Ca^{2+} channels. The LVA Ca^{2+} channels include the Ca_V3 family (also designated α1G, α1H and α1I; Ertel et al., 2000) and are considered Transient/Tiny or T-type Ca^{2+} channels (Tsien et al., 1988; Cribbs et al., 1998). T-type Ca^{2+} channels and HVA Ca^{2+} channels differ in their permeation. For example, T-type Ca^{2+} channels have similar Ca^{2+} and Ba^{2+} unitary conductances, where as the unitary conductance of Ba^{2+} is greater than Ca^{2+} in HVA Ca^{2+} channels (Fukushima & Hagiwara, 1985; Bean, 1985; Carbone & Lux, 1987; Huguenard, 1996). Most of the differences in the permeation properties of T-type Ca^{2+} channels and HVA Ca^{2+} channels have been shown using divalent cations (Lee et al. 1999). However, under physiological conditions both the internal and external environments of channels are dominated by monovalent cations. Therefore, we tested the hypothesis that the permeation properties of T-type Ca^{2+} channels are differently regulated by monovalent cations as well.

In physiological [Ca^{2+}], influx through VGCC is primarily carried by Ca^{2+} ions. This is because of the

*Department of Medicine, The University of Wisconsin, Madison, WI 53706, USA
Correspondence to: J. Satin; email: jsatin1@uky.edu

high-affinity binding of Ca^{2+} to the pore, and the 10^4 concentration gradient of Ca^{2+} across the membrane (McCleskey & Almers, 1985). In contrast, the outward current is predominantly carried by the internal monovalent cation. In symmetrical monovalent conditions, the reversal potential can be used as an indicator to determine how competitive a monovalent ion is with Ca^{2+} for permeating the channel. Monovalent ions that effectively compete with Ca^{2+} will reverse closer to 0 mV when compared to monovalents that weakly compete with Ca^{2+} (Hille, 2001).

We recorded macroscopic currents from the cloned T-type Ca^{2+} channels (α1G and α1H; $Ca_V3.1$ and $Ca_V3.2$) in physiological [Ca^{2+}] to determine how monovalent cations alter the permeation properties of T-type Ca^{2+} channels. We report that, in physiological [Ca^{2+}], external monovalent cations are important determinants of the selectivity of T-type Ca^{2+} channels.

Materials and Methods

Cell Culture

The α subunits of LVA Ca^{2+} channels (α1G and α1H) were cloned and used to generate a stably-transfected HEK 293 cell line provided by Dr. Leanne Cribbs from Loyola University (Cribbs et al., 1998; Zhang, Cribbs & Satin, 2000). Cells were incubated in DMEM, supplemented with 10% fetal bovine serum, with 100 U/ml penicillin, 100 mg/ml streptomycin, and 1 mg/ml G-418 for selection. Heterologous expression of the α subunit in HEK cells provides a model system for recording T-type Ca^{2+} current (I_T) with native-like properties (Satin & Cribbs, 2000). Approximately 90% of the cells tested had I_T; the other 10% had no current and were considered 'blank'. Blank cells had negligible background currents in our recording solutions. Therefore, the HEK cells that heterologously express I_T have a null background.

I_T was measured using the whole-cell voltage-clamp technique, enabling the measurement of net ionic current across the plasma membrane. Current recordings were initiated 5 minutes after patch break to allow equilibration of the pipette solution and the cell's interior. The cells were recorded in a chamber with a static bath volume of 50–250 μl. To change the bath solution, new bath solution was superfused at 8 ml/minute for 1–2 minutes. Flow was stopped for recording in the new bath solution. The solution of the reference electrode was isolated from the bath, and did not change during perfusion. Changes in liquid junction potential were corrected off-line, calculated from the routine provided by pClamp 8.02b (Axon Instruments). Experiments were performed at room temperature (20–22°C). Pipettes were pulled from borosilicate glass with resistances ranging from 1.5 to 2 MΩ. The mean series resistance before compensation was between 2–4 MΩ. Series resistance was compensated between 75 and 90%. Currents were filtered at 10 kHz and sampled at 50 kHz. For all tail-current measurements, the capacitative transient was complete within 100–150 μs. Single exponential functions superimposed the current decay, consistent with a constant V_{test} during the measurement. The time constant of deactivation for a given potential was independent of current amplitude, reflecting good voltage control.

Solutions

Cells were digested with 0.125% trypsin and replated 1–3 days prior to recording. Culture medium was replaced with the extracellular bath solution immediately prior to recording. For recording in conditions with Li^+ or Cs^+ (X), the pipette solution contained (in mM): 140 XCl, 5 Mg-ATP, 5 EGTA, and 10 HEPES. The solutions were titrated with XOH to pH 7.2. The extracellular bath solution consisted of (in mM): 140 XCl, 2.5 $CaCl_2$, 20 glucose, 5 HEPES, and 5 MES. The solutions were titrated with XOH to either pH_o 7.4 or 6.0.

Activation was measured by holding at a maximally available potential of −105 mV followed by a V_{test} between −80 mV to 115 mV for 300 ms. The peak current was plotted as a function of V_{test}. Reversal potential was calculated by linearly extrapolating current amplitudes through the voltage axis. Reversal potential was also measured by pre-pulsing to 40 mV followed by 2.5-mV test steps through the reversal potential. The data and its acquisition in Fig. 7*C* were previously reported in Delisle & Satin (2000). The open *I-V* curve in Fig. 7*C* was generated by stepping to the peak outward current at 100 mV, followed by test steps from −120 mV to 115 mV.

Analysis and Statistics

pClamp6.04 and 8.02b programs (Axon Instruments) were used for data analysis and acquisition. To do statistical comparisons, the data was reported as mean ± SEM (standard error of the mean). Student's *t*-test on planned comparisons was used to evaluate *p* values. Statistical analysis was not done on normalized data sets. Eyring rate simulations were performed using the permeation program provided by Dang & McCleskey (1998) at http://www.ohsu.edu/vollum/mccleskey/. Slight modifications were made to the energy barriers and wells (*see* Fig. 7 legend). The high-affinity binding well was moved from 50% in the electric field to 25%, in accordance with data reported by Kuo & Hess (1993a; 1993b; 1993c).

Results

In Physiological [Ca^{2+}], External Li^+ Modifies Ca^{2+} Selectivity in α1G and α1H

In physiological ionic conditions, the reversal potential of HVA Ca^{2+} channels deviates from the equilibrium potential for Ca^{2+} (E_{Ca}) because monovalent ions also permeate through the channel (Hille, 2001). The reversal potential can be used as an index of channel selectivity when the internal and external ionic concentrations are known. In HVA Ca^{2+} channels the relative permeability X^+/Ca^{2+} ratio is greater for Li^+ than Cs^+ (Hess, Lansman & Tsien, 1986; Tsien et al., 1987). We confirmed this trend in cloned T-type Ca^{2+} channels as well, by recording I_T in symmetrical Li^+ (Li^+/Li^+) and Cs^+ (Cs^+/Cs^+). Figure 1 shows pooled *I-V* relationships recorded from cells expressing cloned T-type Ca^{2+} channels (α1G, *triangles*; α1H, *squares*) in Li^+/Li^+ (Fig. 1*A*) and Cs^+/Cs^+ (Fig. 1*B*). In Li^+/Li^+, the reversal potential was closer to 0 mV compared to Cs^+/Cs^+. In both isoforms, the reversal potential was less than

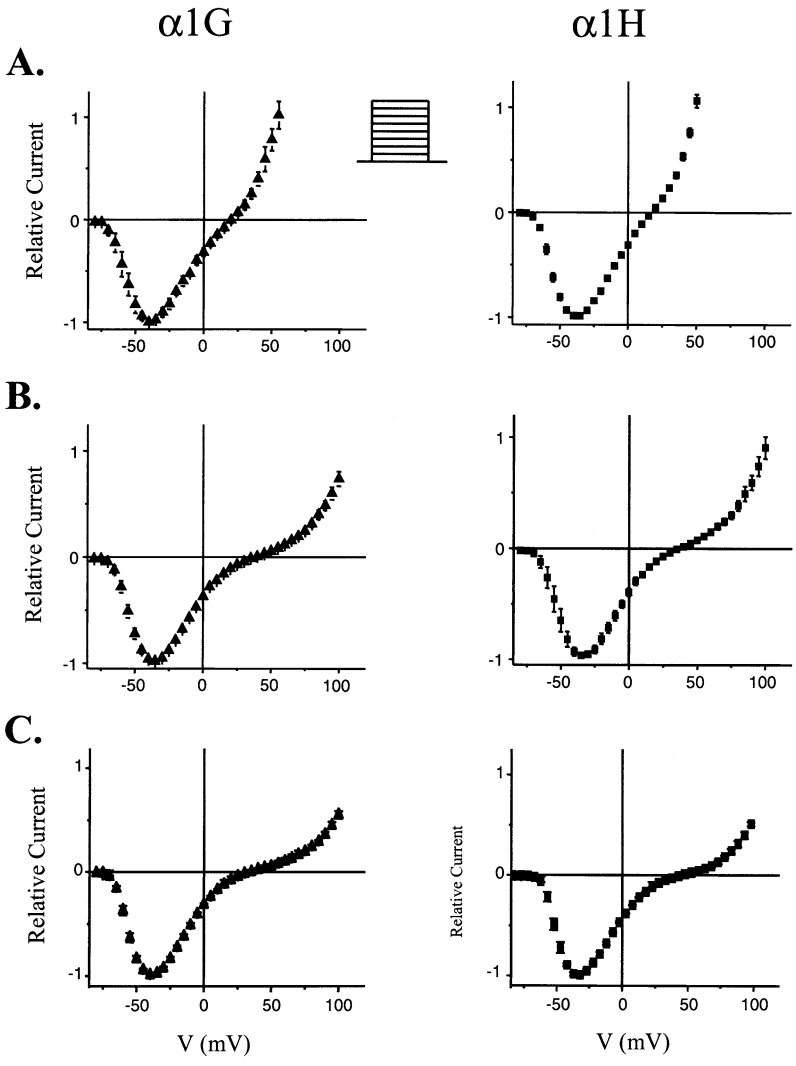

Fig. 1. Li^+ has a higher relative permeability than Cs^+ in cloned LVA Ca^{2+} channels. The relative permeability of Li^+ is greater than that of Cs^+ in HVA Ca^{2+} channels. To test this trend in the cloned LVA Ca^{2+}, we recorded *I-V* relationships in cells expressing α1G (*left panel*) or α1H (*right panel*). The *I-V* relationships were normalized to the peak inward current and averaged ($n = 4$). Mean relative current (± SEM) in (*A*) symmetrical Li^+ (Li^+/Li^+), (*B*) symmetrical Cs^+ (Cs^+/Cs^+), and (*C*) with external Li^+ and internal Cs^+ (Li^+/Cs^+). The reversal potential in $Li^+/Li^+ < Cs^+/Cs^+$, demonstrating that Li^+ has a higher relative permeability than Cs^+.

20 mV in Li^+/Li^+, but between 35 and 40 mV in Cs^+/Cs^+. Thus, Li^+ has a higher permeability than Cs^+ through T-type Ca^{2+} channels.

We wanted to determine if external Li^+ permeates the T-type Ca^{2+} channel in physiological bath [Ca^{2+}]. Figure 1*C* shows the pooled *I-V* relationships recorded from cells expressing α1G (*triangles*) and α1H (*squares*) with Li^+ outside and Cs^+ inside. The reversal potential in Li^+/Cs^+ was more positive than in Cs^+/Cs^+. Figure 2 summarizes the mean reversal potentials measured from the peak *I-V* curves. For both α1G and α1H the reversal potential becomes farther removed from 0 mV in the graded order Li^+/Li^+, Cs^+/Cs^+, and Li^+/Cs^+ (outside/inside). The extreme positive reversal potential of Li^+/Cs^+ demonstrates that in physiological bath [Ca^{2+}], external Li^+ altered T-type Ca^{2+} channel selectivity.

Measuring changes in reversal potential from T-type channel *I-V* relationships can be problematic due to the contamination of gating current (e.g., *see* Burgess et al., 2002) with ionic current. To confirm our measurements from Figs. 1 and 2, we recorded tail currents through the reversal potential in Cs^+/Cs^+ and Li^+/Cs^+. Figure 3*A* shows representative tail currents of α1G at 28.5 mV and 45 mV in Cs^+/Cs^+ and Li^+/Cs^+. Replacement of external Cs^+ with Li^+ prevented the outward tail currents at 45 mV. This effect was reversible with wash back to symmetrical Cs^+. Figure 3*B* plots the mean tail current as a function of test potential for α1G in Cs^+/Cs^+ and Li^+/Cs^+. The mean reversal potential measured from tail currents in Cs^+/Cs^+ was 39 mV in α1G and 40 mV in α1H. Replacement of external Cs^+ with Li^+ shifted the mean reversal potential measured from tail currents to 45 mV in both α1G and α1H (Fig. 3*C*). We also tested the effect of the physiologically relevant monovalent cation Na^+. Switching the bath solution from Li^+/Cs^+ to Na^+/Cs^+ resulted in only a negligibly different mean reversal potential (mean difference 0.4 mV).

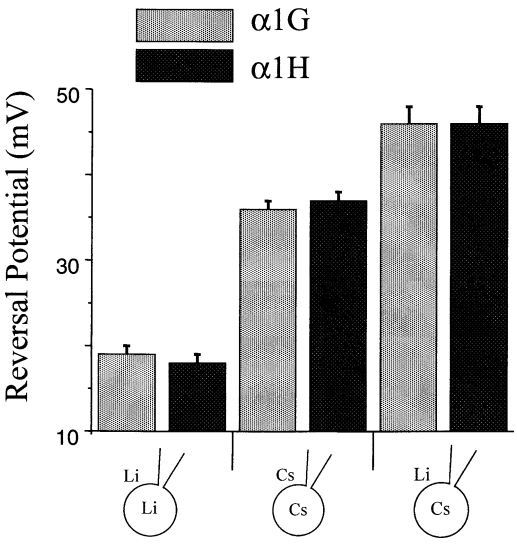

Fig. 2. Summary of reversal potential data from peak *I-V* curves. T-type Ca channels follow L-type monovalent sequence of relative permeability, Li^+ being more permeant than Cs^+. However, external Li^+/internal Cs^+ shows more positive reversal potential. $n = 4$ α1H and α1G, mean ± SEM.

Replacement of External Cs^+ with Li^+ Increases Inward Tail Currents

Figure 1 demonstrates that Li^+ has a higher relative permeability than Cs^+. Moreover, the positive shift of reversal potential with external replacement of Cs^+ with Li^+ shows that external Li^+ can alter Ca^{2+} channel selectivity. We next wanted to determine if external Li^+ modifies T-type Ca^{2+} channel selectivity via influx through the channel. We generated an open-channel *I-V* curve by measuring current amplitude at various potentials following a pre-pulse to a maximally activating voltage step. This procedure enforces a constant nP_o, allowing measurement of relative permeability across a broad voltage range. The pre-pulse was followed by test steps ranging from −157.5 mV to +120 mV. Note that the slight differences in V_{test} between symmetrical Cs^+ and with external Li^+ and internal Cs^+ were due to changes in the liquid junction potential. (Since the reference electrode was isolated from the bath using a salt bridge, changes in the liquid junction potential were made off-line using pClamp 8.2.) For very large negative test potentials the inward tail currents were too large to measure reliably. To circumvent this problem we increased duration of the pre-pulse to inactivate a fraction of channels. The voltage-independent τ_{inact} (i.e., the $\tau_{inact,max}$) was not significantly different in either Cs^+/Cs^+ (22 ± 2 ms) or Li^+/Cs^+ (23 ± 2 ms) for α1G (Fig. 4*A*). We recorded peak tail I_T after pre-pulsing for 22 ms, thus allowing for a substantial but constant degree of open-channel inactivation during the pre-pulse. Given the constancy of the inactivation time course, the relative fraction of channels that will be open at the end of the pre-pulse will be the same in either Cs^+/Cs^+ or Li^+/Cs^+. Figure 4*B* shows representative tail currents for α1G at −150 mV in Cs^+/Cs^+ and −147.5 mV in Li^+/Cs^+. The tail current decays were well described by a single exponential (white line). External replacement of Cs^+ with Li^+ increased peak tail current for negative potentials. Figure 4*C* shows the pooled open-channel *I-V* relationship for α1G in Cs^+/Cs^+ and Li^+/Cs^+. The data demonstrate that the substitution of external Cs^+ with the more permeant Li^+ increased inward current. We conclude that external replacement of Cs^+ with Li^+ alters T-type Ca^{2+} channel selectivity and increases the external monovalent influx.

α1H's Ca^{2+} Selectivity Is more Sensitive to External Acidification than α1G

The data in Fig. 4 demonstrates that increasing the relative permeability of the external monovalent ion increases inward current in physiological $[Ca^{2+}]$. We previously reported that external $[H^+]$ also alters the Ca^{2+} channel selectivity in α1H (Delisle & Satin, 2000). Figure 5*A* shows pooled *I-V* data in Li^+/Cs^+ for α1G. The data were normalized to the peak inward current in pH_o 7.4. Similar to other voltage-gated Ca^{2+} channels, external acidification from pH_o 7.4 to 6.0 caused a positive translation of the *I-V* relationship and a decrease in the inward current. The reduction of inward current is primarily due to H^+ modification of activation gating (Tytgat, Nilius & Carmeliet, 1990; Delisle & Satin, 2000). For large test potentials, where the probability of channel opening approaches maximal, there is no significant difference in the outward currents in pH_o 6.0 or pH_o 7.4. Figure 5*B* shows pooled *I-V* relationships from cells expressing α1H. The data were normalized to the peak inward current in pH_o 7.4. Unlike α1G, the outward currents are larger in pH_o 6.0 compared to pH_o 7.4. Below are representative tail current traces recorded at test potentials through reversal potential for α1G (Fig. 5*C*) and α1H (Fig. 5*D*). At pH_o 6.0 the outward tail currents are larger and reverse at a more negative potential for α1H, but not α1G. The negative shift of reversal potential in α1H is reversible with wash back to pH_o 7.4. The mean reversal potential for α1H shifted from 45 ± 2 mV at pH_o 7.4 to 37 ± 2 mV at pH_o 6.0 ($p < 0.05$). The data demonstrate that the Ca^{2+} selectivity in α1H is more sensitive to modification by external $[H^+]$ than α1G.

Internal Li^+ Blunts the H^+ Modification of α1H's Selectivity

α1H's reversal potential shifted negative 8 mV in pH_o 6.0 compared to pH_o 7.4. This indicated that

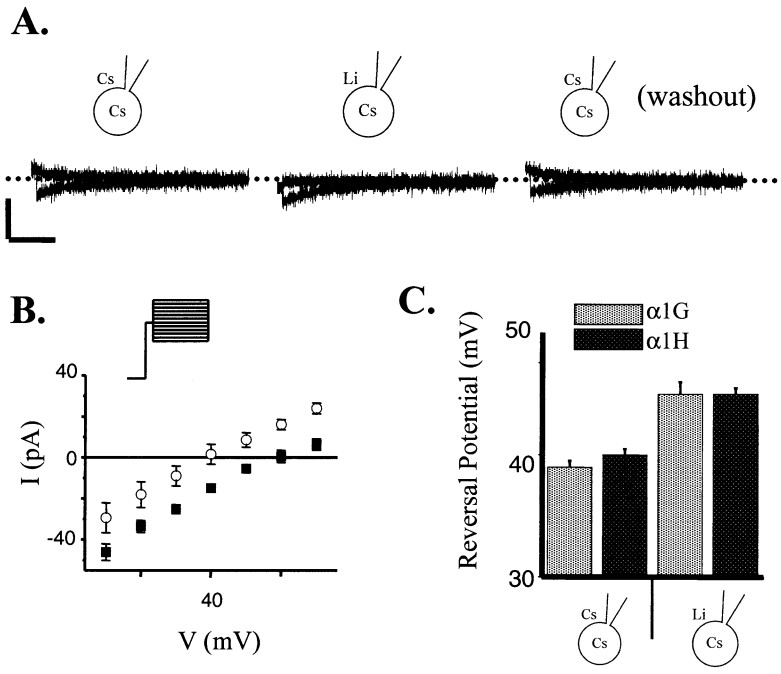

Fig. 3. In symmetrical Cs^+, replacement of external Cs^+ with Li^+ causes a shift of reversal potential towards E_{Li}. (*A*) Representative currents for α1G recorded at 28.5 mV and 45 mV in Cs^+/Cs^+. Li^+/Cs^+, and wash back to Cs^+/Cs^+. External Li^+ blocked outward current at 45 mV, and was reversible with wash back to Cs^+/Cs^+. (*B*) A plot of the mean tail current amplitudes recorded from 4 cells expressing α1G shows that external Li^+ shifted the reversal potential towards E_{Li}. Cs^+/Cs^+ (*circles*); Li^+/Cs^+ (*squares*) Scale bars, 100 pA and 20 ms. (*C*) The mean reversal potentials, calculated from tail currents, for α1G (*light grey*) and α1H (*dark grey*) were 39 mV and 40 mV in Cs^+/Cs^+. External replacement of Li^+ with Cs^+ shifted the mean reversal potential to 45 mV in both isoforms ($n = 4$).

acidification reduced either the permeability of external Li^+ or Ca^{2+}. In other words, acidification appears to increase the relative permeability of the internal monovalent cation. If acidification does increase the relative permeability of the internal ion, then altering the permeability of the internal ion should alter the pH_o-induced shift of reversal potential (Fig. 1*A*-1*B*). Figure 6*A* shows pooled *I-V* data recorded with internal Li^+ in pH_o 7.4 (*squares*) and pH_o 6.0 (*circles*). Similar to Figs. 5*A* and 5*B*, acidification from pH_o 7.4 to 6.0 caused a positive translation of the *I-V* relationship and a reduction in the inward current. In contrast to Fig. 5*B*, the outward currents at pH_o 6.0 were not larger than at pH_o 7.4. In Fig. 6*B* we plotted the mean reversal potential for pH_o 7.4 and 6.0 in Li^+/Li^+ and with internal Cs^+ (Li^+/Cs^+). The data demonstrate that internal Li^+, which has a higher relative permeability than Cs^+, blunted the effects of external acidification on T-type Ca^{2+} channel selectivity. Therefore we conclude that increasing external $[H^+]$ reduces external cation influx, and effectively allows an increase in the relative permeability of the internal monovalent cation. Internal ions that have a higher relative permeability blunt the effect of acidification on T-type Ca^{2+}-channel selectivity.

Discussion

External Monvalent Cations Regulate LVA Ca^{2+} Channel Selectivity

This paper reports the novel finding that, under conditions of physiological bath $[Ca^{2+}]$, external monovalent cations are important determinants to the selectivity of T-type Ca^{2+} channels. There is a relationship between the absolute permeability of a given external monovalent cation and T-type Ca^{2+} channel selectivity. Replacing a weakly permeant external monovalent cation, Cs^+, with a more permeant one, Li^+, resulted in a positive shift of reversal potential, and concomitantly an increase of inward current. The increase of inward current is not simply due to additional driving force for a given negative potential. Rather, the open-channel *I-V* relationship suggests that monovalent conductance of the highly permeant species contributes to the net inward current for hyperpolarized potentials. In other words, we show that the inward I_T, in physiological bath $[Ca^{2+}]$, is carried by a mixture of Ca^{2+} and monovalent cations.

External Monovalent Regulation of HVA and T-type Ca^{2+} Channels

By recording in physiological $[Ca^{2+}]$ and symmetrical monovalent conditions, we determined that the relative permeability of Li^+ is greater than that of Cs^+. Replacing external Cs^+ with Li^+ caused a positive shift of reversal potential, and increased macroscopic tail currents when Cs^+ was used in the pipette. Taken together the data suggest that external Li^+ modifies T-type Ca^{2+} channel selectivity by flowing inward through the channel.

The influx of external monovalent cations in physiological $[Ca^{2+}]$ contrasts the previous reports in studies concerning HVA Ca^{2+} channels. Yamashita, Ciani & Hagiwara (1990) and Polo-Parada & Korn

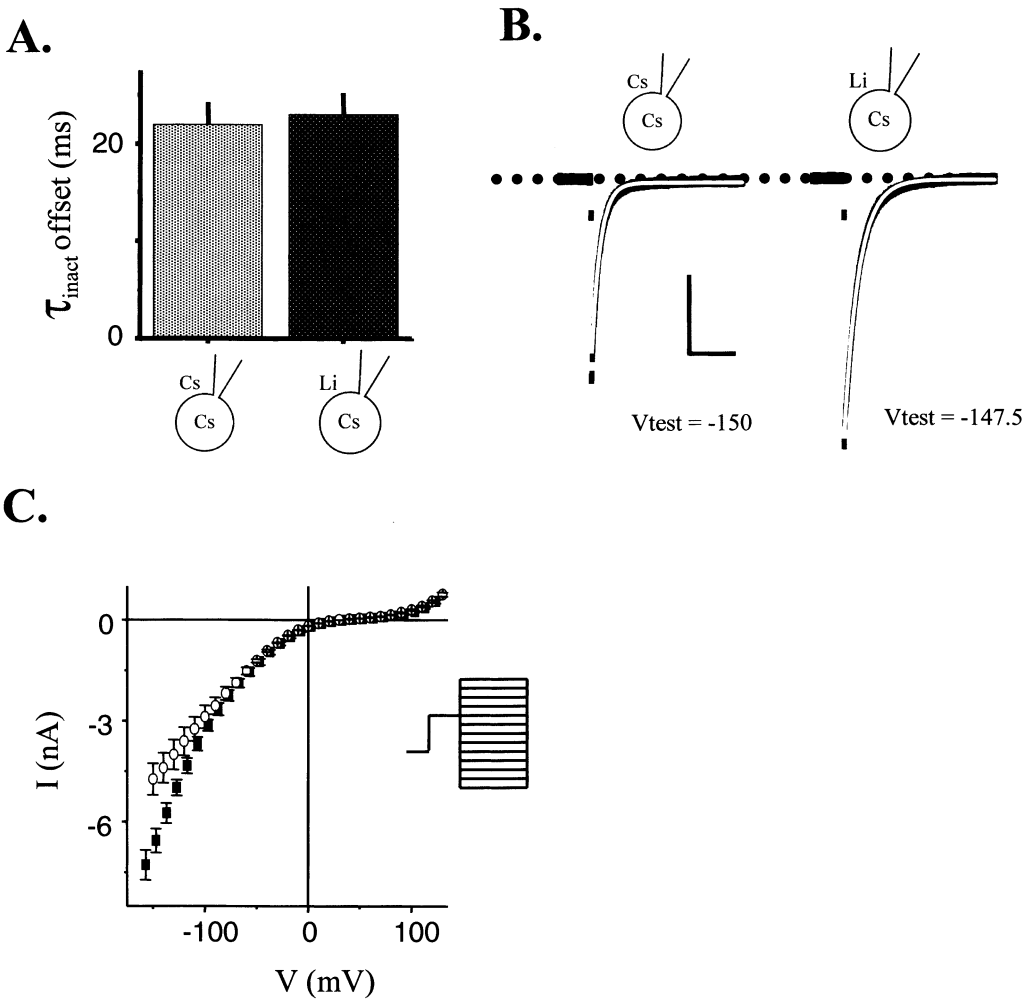

Fig. 4. Replacement of external Cs^+ with Li^+ increased Inward current. We normalized nP_o by pre-pulsing cells to potentials approaching maximal activation and recorded tail currents from −157 mV to +125 mV. The pre-pulse duration was set to the voltage-independent τ_{inact} for α1G. Scale bars 2 nA and 5 ms. (*A*) Replacement of external Cs^+ with Li^+ did not alter the voltage-independent τ_{inact} ($\tau_{inact,max}$) in α1G; the mean τ_{inact} in Cs^+/Cs^+ was 22 ± 2 ms in Cs^+/Cs^+ and 23 ± 2 ms in Li^+/Cs^+. (*B*) Tail currents (*rectangular dots*) recorded from a representative cell show that the peak current is smaller at −150 mV in Cs^+/Cs^+, than the peak tail current at −147.5 after external replacement of Cs^+ with Li^+. Single exponential functions (*white lines*) superimposed the current decay, consistent with voltage control. (*C*) A plot of mean tail current amplitudes recorded from cells expressing α1G in Cs^+/Cs^+ (*circles*) and Li^+/Cs^+ (*squares*). External replacement of Cs^+ with Li^+ increased peak inward tail currents (n = 4).

(1997) showed that increasing the external Na^+/NMG^+ or Na^+/TEA^+ ratio had no effect on Ca^{2+} selectivity. Our results are the first to show that external monovalent cations can regulate Ca^{2+} selectivity in physiological [Ca^{2+}]. Yamashita et al. (1990) reported that increasing the Na^+/NMG^+ ratio did not alter inward currents from native HVA Ca^{2+} channels. However, Polo-Parada & Korn (1997) showed that increasing the external Na^+/TEA^+ ratio blocked inward Ca^{2+} current in native HVA Ca^{2+} channels. We show for the first time that increasing the permeability of the external monovalent cations can actually *increase* inward current through T-type Ca^{2+} channels. Our results may differ from the previous reports on monovalent regulation of VGCC because of differences in the pore properties of T-type Ca^{2+} channels compared to HVA Ca^{2+} channels. Our results may also differ because of the differences in the internal and external ionic conditions. It should be noted, however, that we obtain similar reversal potentials with for Li^+/Cs^+ as for Na^+/Cs^+. Thus, it is likely that the most important difference between our study and previous studies is that we used weakly permeant cations in the pipette. Yamashita et al. (1990) used Na^+ in the pipette, whereas Polo-Parada et al. (1997) primarily used impermeant ions in the pipette.

External [H^+] Regulation of HVA and T-type Ca^{2+} Channels

External acidification reduces Ca^{2+} influx in HVA Ca^{2+} channels, without altering selectivity (Kwan &

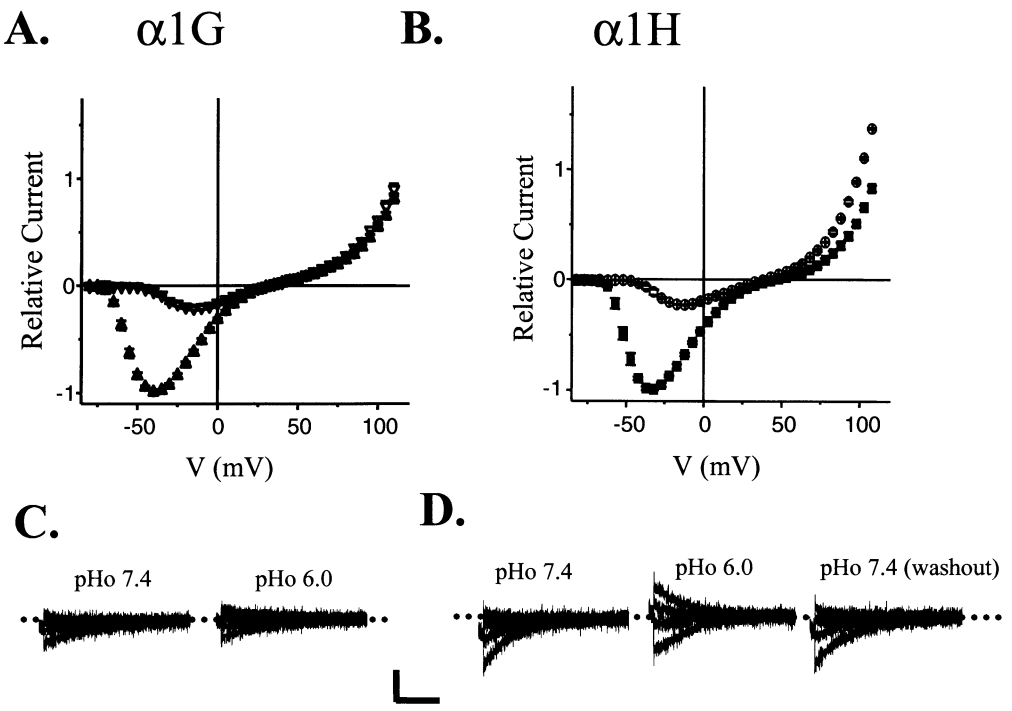

Fig. 5. External acidification from pH_o 7.4 to pH_o 6.0 decreased external cation selectivity in α1H. (*A*) Pooled *I-V* relationships for α1G and (*B*) α1H in Li^+/Cs^+ were normalized to the peak inward current in pH_o 7.4 (*solid symbols*). External acidification to pH_o 6.0 (*open symbols*) caused a positive translation of the *I-V* relationship, and reduced inward currents in both α1G and α1H. Acidification selectively increased outward currents in α1H. (*C*) Selected raw tail current traces between 25 and 45 mV for α1G and (*D*) α1H in pH_o 7.4 and 6.0. External acidification to pH_o 6.0 did not alter current around reversal potential in α1G. In contrast, acidification resulted in an outward tail current in α1H at 45 mV. Scale bars 75 pA and 15 ms.

Kass, 1993; Pietrobon, Prod'hom & Hess, 1989; Tombough & Somjen, 1996; Zhou & Jones, 1996). In contrast, increasing external $[H^+]$ reduced external cation selectivity in α1H, resulting in a negative shift of reversal potential. Replacement of internal Cs^+ with Li^+ reduced the negative shift of reversal potential with acidification. The data also demonstrate that internal monovalent cations with a higher relative permeability blunt the effect of external $[H^+]$ on external cation selectivity. Thus it is likely that residues involved with the ion permeation pathway mediate the unique proton regulation of T-type channels. Given that T-type and HVA channels lack identity throughout the permeation pathway it is plausible that structural differences account for the disparate H^+ regulation of HVA and T-type Ca^{2+} channel permeation.

It has been widely suggested that at high external $[H^+]$, H^+ may titrate acidic residues external to the selectivity filter that are important for the dehydration of ions in HVA Ca^{2+} channels (Prod'hom, Pietrobon & Hess, 1989; Kuo & Hess, 1993c). We wanted to determine if the effects of external acidification on the selectivity of α1H could be reproduced using an Eyring rate model. We slightly modified the Eyring rate of Ca^{2+} ions proposed for HVA Ca^{2+} channels by Dang and McCleskey (1997), because the outer energy barriers are thought to partly represent the energy associated with cation dehydration. The high-affinity binding well was moved from 50% in the electric field to 25%, in accordance with data reported by Kuo & Hess (1993a, 1993b, 1993c). To mimic the increase in the energy of Ca^{2+} dehydration we selectively raised the outer energy barrier by 2 *RT* units. Figure 7*A* shows the energy profile of Ca^{2+} at an alkaline pH (*solid line*) and at an acidic pH (*dotted line*). The inset shows the energy profile we used for the monovalent ions. For simplification we restricted ourselves to changing only the outermost energy barrier of the Ca^{2+} energy profile. Figure 7*B* shows the open *I-V* curve calculated by the model, using a $[Ca^{2+}]$ of 2.5 mM and a [monovalent] of 140 mM for both the alkaline energy profile (*squares*) and the acidic energy profile (*circles*). Figure 7*C* is an open *I-V* curve that was recorded in mixed ionic conditions from α1H at pH 8.2 (*squares*) and 5.5 (*circles*) previously reported in Delisle and Satin (2000). The model recapitulates 3 important observations from the data: 1) the outward current is larger at acidic pH; 2) the shift to more negative potentials at acidic pH; and 3) the inward currents at acidic pH cross over and become larger than the inward currents at alkaline pH.

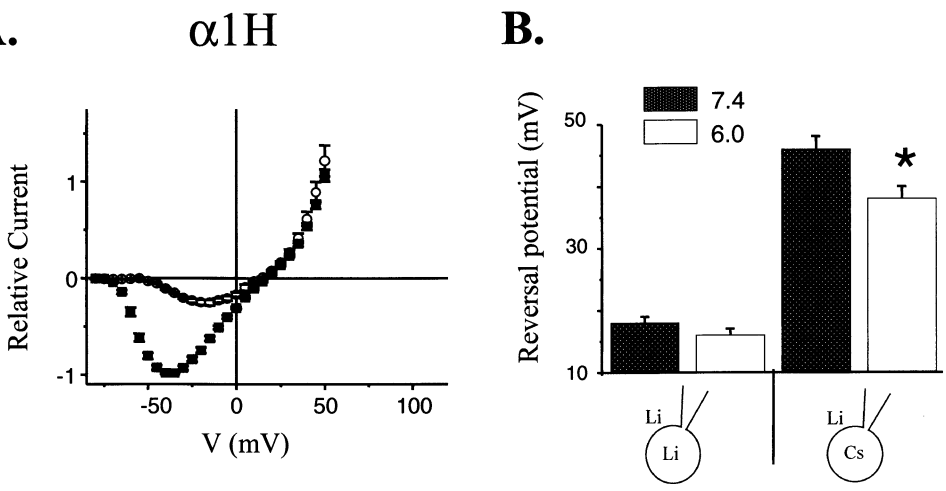

Fig. 6. Internal Li^+ blunts the acidification-induced shift of reversal potential for α1H. (*A*) Pooled *I-V* relationships for α1H in Li^+/Li^+ at pH_o 7.4 and 6.0. Data were normalized to the peak inward current in pH_o 7.4. Similar to Fig. 5, external acidification caused a positive translation of the *I-V* relationship and reduced inward current. In contrast to Fig. 5*B*, the outward current was not different in pH_o 7.4 or 6.0. (*B*) The mean reversal potential significantly shifted negative with internal Cs^+, but not with internal Li^+ ($*p < 0.05$).

Isoform Differences in pH_o Regulation of LVA Ca^{2+} Channel Selectivity

The sensitivity of LVA Ca^{2+} channel selectivity to external pH_o was isoform-specific. α1H was more sensitive to H^+ modification of selectivity than was α1G. The selectivity of α1G was also reduced by increasing external $[H^+]$, but only at a higher external $[H^+]$ (*data not shown*). A difference in the permeation properties between the α1G and α1H isoforms is not a novel observation. These isoforms also differ in their sensitivity to external Ni^{2+} blockade. Similar to changes in external $[H^+]$, α1H is also more sensitive to Ni^{2+} blockade compared to α1G (Lee et al., 1999). The difference between isoform sensitivity may represent subtle structural differences in the pore. It is unlikely that the differences are related to the relative permeability of the monovalent cations, because the reversal potentials under symmetrical and bi-ionic conditions are so similar (Fig. 2).

In contrast to effects on selectivity, proton-induced changes of inward current and the positive-shift *I-V* relationship in α1G and α1H were almost identical (Fig. 4). We previously showed that the proton-induced reduction of cloned T-type Ca^{2+} channel current is due to changes in the voltage dependence of channel activation and not due to H^+ block of macroscopic current (Delisle & Satin, 2000). In comparing the pH effects on the two isoforms, there is discordance between the effects on selectivity (only on α1H) and channel activation (Fig. 5). Similarly, replacement of internal Cs^+ with Li^+ blunted the effect of external acidification on selectivity but not channel activation in α1H (Figs. 5–6). These results demonstrate that H^+ modification of T-type Ca^{2+} channel gating is independent of H^+ modification of T-type Ca^{2+} channel selectivity.

Physiological Implications: Regulation of Ca^{2+} Influx via Selectivity

Our data demonstrate that the selectivity of T-type Ca^{2+} channels is dependent on both the internal and external monovalent cations. We report the novel finding that in contrast to HVA Ca^{2+} channels, external monovalent cations can regulate T-type Ca^{2+} channel selectivity. There are conflicting reports on the regulation of HVA Ca^{2+} current by external Na^+. Yamashita et al. (1990) recorded I_{HVA} in lymphocytes and concluded that increasing the external Na^+/NMG^+ ratio does not alter Ca^{2+} influx. In contrast, Polo-Parada and Korn (1997) recorded I_{HVA} in neurons, and concluded that external Na^+ reduces Ca^{2+} influx by ~50%. Both these papers support the notion that external Na^+ does not alter HVA Ca^{2+} channel selectivity in physiological $[Ca^{2+}]$. In contrast, we report the novel observation that external Li^+ does alter T-type Ca^{2+} channel selectivity and actually *increases* inward current through T-type Ca^{2+} channels under conditions of physiological bath $[Ca^{2+}]$, highly permeant external monovalent cation (such as Na^+ or Li^+), and a weakly permeant internal monovalent cation.

Our results demonstrate that external Li^+ can contribute to ionic influx in LVA Ca^{2+} channels. We suggest that in physiological ionic conditions, external Na^+ may also regulate T-type Ca^{2+} channel selectivity by permeating through the channel. Therefore, unlike HVA Ca^{2+} channels, macroscopic current through LVA Ca^{2+} channels may contain a mixture of Na^+ and Ca^{2+}. This may

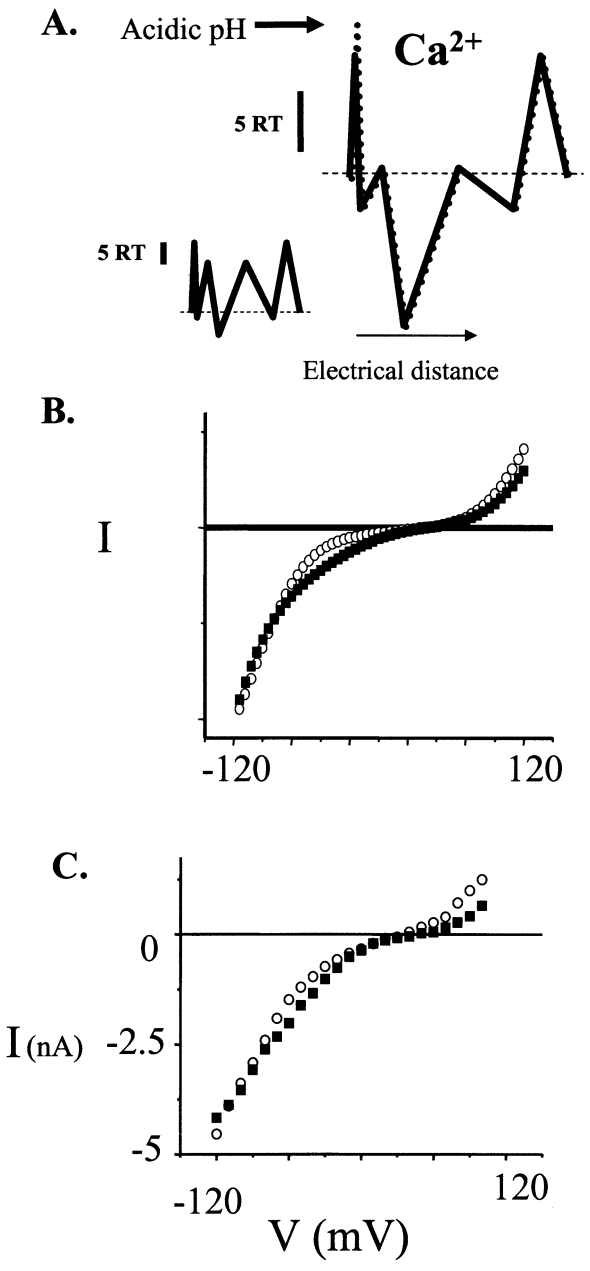

Fig. 7. Erying rate theory suggests that external acidification increases the energy of dehydration of Ca^{2+} for α1H. (*A*) An Erying rate model for Ca^{2+} in alkaline pH (*solid line*) and at acidic pH (*dotted line*). We raised the outermost energy barrier 2 RT units to mimic an increase in the energy of dehydration. The inset shows the energy profile of the monovalent cation. (*B*) The open *I-V* of the Erying rate model with 140 mM monovalent on either side and an external [Ca^{2+}] of 2.5 mM. (*C*) open-channel *I-V* recorded from α1H in mixed ionic conditions. The model recapitulates the effects of acidification on the open-channel *I-V* recorded from α1H (Delisle & Satin 2000).

be particularly relevant in mutant thalamic neurons containing enhanced LVA Ca^{2+} channel activity (Zhang et al., 2002). Enhanced LVA Ca^{2+} tail currents, such as those that occur during the rapid repolarization of the action potential, may alter Na^+ and Ca^{2+} homeostasis as well as membrane excitability. Finally, consider the events that accompany ischemia. At low tissue pH our results predict that Na^+ flux becomes greater via T-type Ca^{2+} channels. Thus, increased Na^+ entry via T-type Ca channels may contribute to allodynia in response to local acidification. In the case of myocytes, the increased Na^+ entry decreases the effectiveness of NCX and thus can contribute to decreased lusitropy in pathological heart muscle. In conclusion, therapy for allodynia should include consideration of T-type Ca channel blockade.

We are grateful to the continuing support with cells and clones by Dr. L.L. Cribbs (Loyola). Supported by NIH HL-63416 (J.S.). JS is an Established Investigator of the American Heart Association.

References

Bean, B.P. 1985. Two kinds of calcium channels in canine atrial cells: differences in kinetics, selectivity, and pharmacology. *J. Gen. Physiol.* **86:**1–30

Burgess, D.E., Crawford, O., Delisle, B.P., Satin, J. 2002. Mechanism of inactivation gating of human T-type (low-voltage activated) calcium channels. *Biophys. J.* **82:**1894–1906

Carbone, E., Lux, H.D. 1987. Kinetics and selectivity of a low-voltage-activated calcium current in chick and rat sensory neurones. *J. Physiol.* **386:**547–570

Cribbs, L.L., Lee, J.-H., Yang, J., Satin, J., Zhang, Y., Daud, A., Barclay, J., Williamson, M.P., Fox, M., Rees, M., Perez-Reyes, E. 1998. Cloning and characterization of α1H from human heart, a member of the T-type calcium channel gene family. *Circ. Res.* **83:**103–109

Dang, T.X., McCleskey, E.W. 1998. Ion channel selectivity through stepwise changes in binding affinity. *J. Gen. Physiol.* **111:**185–193

Delisle, B.P., Satin, J. 2000. pH Modification of human T-type calcium channel gating. *Biophys. J.* **78:**1895–1905

Ertel, E.A., Campbell, K.P., Harpold, M.M., Hofmann, F., Mori, Y., Perez-Reyes, E., Schwartz, A., Snutch, T.P., Tanabe, T., Birnbaumer, L., Tsien, R.W., Catterall, W.A. 2000. Nomenclature of voltage-gated calcium channels. *Neuron* **25:**533–535

Fukushima, Y., Hagiwara, S. 1985. Currents carried by monovalent cations through calcium channels in mouse neoplastic B lymphocytes. *J. Physiol.* **358:**255–284

Hess, P., Lansman, J.B., Tsien, R.W. 1986. Calcium channel selectivity for divalent and monovalent cations: voltage and concentration dependence of single channel current in ventricular heart cells. *J. Gen. Physiol.* **88:**293–319

Hille, B. 2001. Ion Channels of Excitable Membranes. Sinauer Associates, Inc., Sunderland, MA

Huguenard, JR. 1996. Low-threshold calcium currents in central nervous system neurons. *Annu. Rev. Physiol.* **58:**329–348

Kuo, C.C., Hess, P. 1993a. Block of the L-type Ca^{2+} channel pore by external and internal Mg^{2+} in rat phaeochromocytoma cells. *J. Physiol.* **466:**683–706

Kuo, C.C., Hess, P. 1993b. Characterization of the high-affinity Ca^{2+} binding sites on the L-type Ca^{2+} channel pore in rat phaeochromocytoma cells. *J. Physiol.* **466:**657–682

Kuo, C.C., Hess, P. 1993c. Ion permeation through the L-type Ca^{2+} channel in rat phaeochromocytoma cells: Two sets of ion binding sites in the pore. *J. Physiol.* **466:**629–655

Kwan, Y.W., Kass, R.S. 1993. Interactions between protons and calcium near L-type calcium channels: Evidence for independent channel-associated binding sites. *Biophys. J.* **65:**1188–1195

Lee, J.-H., Gomora, J.C., Cribbs, L.L., Perez-Reyes, E. 1999. Nickel block of three cloned T-type calcium channels: Low concentrations selectively block alpha 1H. *Biophys. J.* **77:**3034–3042

McCleskey, E.W., Almers, W. 1985. The Ca channel in skeletal muscle is a large pore. *Proc. Natl. Acad. Sci. USA* **82:**7149–7153

Pietrobon, D., Prod'hom, B., Hess, P. 1989. Interactions of protons with single open L-type calcium channels. *J. Gen. Physiol.* **94:**1–21

Polo-Parada, L., Korn, S.J. 1997. Block of N-type calcium channels in chick sensory neurons by external sodium. *J. Gen. Physiol.* **109:**693–702

Prod'hom, B., Pietrobon, D., Hess, P. 1989. Interactions of protons with single open L-type calcium channels. Location of protonation site and dependence of proton-induced current fluctuations on concentration and species of permeant ion. *J. Gen. Physiol.* **94:**23–42

Satin, J., Cribbs, L.L. 2000. Identification of a T-type calcium channel isoform in murine atrial myocytes (AT-1). *Circ. Res.* **86:**636–642

Tombough, G.C., Somjen, G.G. 1996. Effects of extracellular pH on voltage gated Na, K, and Ca currents in isolated rat CA1 neurons. *J. Physiol.* **493:**719–732

Tsien, R.W., Hess, P., McCleksky, E.W., Rosenberg, R.L. 1987. Calcium channels: Mechanisms of selectivity, permeation, and block. *Annu. Rev. Biophys. Biophys. Chem.* **16:**265–290

Tsien, R.W., Lipscombe, D., Madison, D.V., Bley, K.R., Fox, A.P. 1988. Multiple types of neuronal calcium channels and their selective modulation. *Trends Neurosci.* **11:**431–438

Tytgat, J., Nilius, B., Carmeliet, E. 1990. Modulation of the T-type cardiac Ca channel by changes in proton concentration. *J. Gen. Physiol.* **96:**973–990

Yamashita, N., Ciani, S., Hagiwara, S. 1990. Effects of internal Na on the Ca channel outward current in mouse neoplastic B lymphocytes. *J. Gen. Physiol* **96:**559–579

Zhang, Y., Cribbs, L.L., Satin, J. 2000. Arachidonic acid modulation of α1H, a cloned human T-type calcium channel. *Amer. J. Physiol.* **278:**H184–H193

Zhang, Y., Mori, M., Burgess, D.L., Noebels, J.L. 2002. Mutations in high-voltage-activated calcium channel genes stimulate low-voltage-activated currents in mouse thalamic relay neurons. *J. Neurosci.* **22:**6362–6371

Zhou, W., Jones, S. 1996. The effects of external pH on calcium channel currents in bullfrog sympathetic neurons. *Biophys. J.* **70:**1326–1334